Nanoscale

ROYAL SOCIETY OF CHEMISTRY

COMMUNICATION

View Article Online
View Journal | View Issue

Cite this: *Nanoscale*, 2021, **13**, 15590

Received 27th May 2021,
Accepted 28th August 2021

DOI: 10.1039/d1nr03408a

rsc.li/nanoscale

Unprecedented neptunyl(v) cation-directed structural variations in Np_2O_x compounds†

Zhong-Fei Xu,‡[a,b] Wen-Jing Zhang,‡[a,b] Ping Zhang[b] and Shu-Xian Hu *[a,b]

Studies on transuranic oxides provide a particularly valuable insight into chemical bonding in actinide compounds, in which subtle differences between metal ions and oxygen atoms are of fundamental importance for the stability of these compounds as well as their existence. In the case of neptunium, it is still mainly limited to specific Np oxide compounds without periodicity in the formation of stable structures or different oxidation states. Here, we report a systematic global minimum search of Np_2O_x (x = 1–7) clusters and the computational study of their electronic structures and chemical bonding. These studies suggest that Np(v) ion could play the structure-directing role, and thus the mixed-valent Np(iii/v) in Np_2O_4 is predicted accessible. In comparison with lower oxidation state Np analogues, significant 5f-orbital covalent interactions with Np(v)=O bonding are observed, which shows that these model neptunium oxides can provide new understandings into the behavior of 5f-electrons in chemical bonding and structural design.

1. Introduction

Nanoscience sometimes produces results that are more mystifying than in any other discipline. Acceptably, neptunium is one of the most complex and fascinating chemical elements in the periodic table.[1] Changes in neptunium dioxide (NpO_2) particle size from bulk to nanoparticles (NPs) could have a dramatic effect on NpO_2 properties. In different solution environments, Np has been known to exist and even co-exist in several oxidation states, from Np(iii) to Np(vii).[1c,2] Among those oxidation states, the pentavalent neputonium within the NpO_2^+ cation is the most widely concerned neptunium species both in nuclear reprocessing technology and under environmentally relevant conditions.[2,3] Recently, it was repeatedly found that neptunium oxide NPs are produced during nuclear waste processing under oxidizing conditions, and formed in interfacial processes between neptunium of different initial oxidation states and various mineral surfaces, and found as bonded to mineral or organic colloids in the groundwater.[4] All these results indicate the high importance of neptunium oxide NPs in the context of the environmental behavior of neptunium. A complete understanding of neptunium oxides at a fundamental level is therefore essential if one is to design future nuclear waste remediation and separation cycles, as well as to develop advanced fuel cycles. Quantum chemistry methods can be used to study radioactive neptunium safely *via* the geometry structure and the electronic structure of such NPs.[5]

Small neptunium oxide clusters can be prepared by laser ablation of neptunium metal in the presence of an oxygen-saturated atmosphere. In the presence of oxygen gas, neptunium oxide clusters such as NpO_2 and Np_2O_5 have already been generated and detected.[6] Several experimental studies have already been applied to study the structural, energetic, vibrational, electronic, and magnetic properties of neptunium oxide clusters.[3a,7] For example, the photoionization spectra of NpO_x were measured and strongly size-dependent ionization potentials were observed.[8] For the NpO_2 molecule, the electron–spin resonance and optical spectroscopy in neon and argon matrices revealed that its ground state is a $^2\Delta$ state, and the molecular bond length and vibrational frequency have been predicted to be 1.761 Å and 942 cm^{-1},[9] respectively. Accompanying these experimental results, several theoretical calculations were also performed to explore the ground-state electronic structures of neptunium oxide clusters,[10] however, most of those studies were mostly focused on the monomer neptunium oxide clusters.[11] In this paper, we systematically study the atomic and electronic structures of neutral dimer Np oxide clusters, which provide more conclusive properties of Np materials with a systematic oxidation state than the monomer species.

[a]*Department of Physics, University of Science and Technology Beijing, Beijing 100083, China. E-mail: hushuxian@csrc.ac.cn*
[b]*Beijing Computational Science Research Center, Beijing, 100193, China*
†Electronic supplementary information (ESI) available. See DOI: 10.1039/d1nr03408a
‡These two authors contributed equally to this work.

2. Results and discussion

2.1. Electronic structure and oxidation state in new neptunium complexes

The most intriguing question concerning Np_2O_x nanoparticles is the potential presence of various oxidation states of neptunium. Global minimum searching by using particle-swarm optimization methodologies based Crystal Structure Analysis in Particle Swarm Optimization (CALYPSO) code[12] combined with full geometry optimization performed at DFT levels (GGA+*U* and PBE/TZ2P)[13] were firstly carried out and followed by DLPNOCCSD(T)[14] energy corrections to predict the ground-state structures corresponding to each potential energy profiles. Based on the most stable structure, which is shown in Fig. 1, the electronic structure, and chemical bonding analyses were further explored. The series of Np_2O_x molecules are fascinating for at least three reasons: (1) each lowest-energy structure appears to be the primary product of the reaction between two Np atoms and the oxygen atoms. (2) They are the simplest examples of a series of complexes with fully distributed oxidation states of Np, *e.g.* Np(I), Np(II) or Np(VII) is a highly unusual oxidation state of Np.[15] (3) One more interesting aspects of this work are the apparent production of several fundamental new molecules of Np, including the Np(II) complex Np_2O_2 in addition to the mix-valent Np(V/III) complex Np_2O_4, and the heptavalent Np oxide Np_2O_7. To address some of these matters, we have delved more deeply into the electronic structure of and bonding in these Np_2O_x complexes.

The ground electron configuration of an Np atom is $[R_n]$ $7s^26d^15f^4$. As known, neptunium could exhibit six oxidation states in molecular complexes, from +2 to +7, with +5 being the most common in aqueous media, although the accessibility of divalent oxidation state requires skillful efforts. An Np(I) complex could, in principle, retain its two metal-based electrons in an s^2f^4, an s^1f^5, or an $s^1d^1f^4$ configuration. The relative energies of the 7s, 6d, and 5f orbitals in a low-valent early-actinide complex will be sensitive to the ligands present. For example, the ligand field provided by three substituted cyclopentadienyl ligands causes U(II) complexes $[U[(^{Ad,Me}ArO)_3mes]^-$ to have an f^4 configuration,[16] in contrast to the $5f^36d^1$ configuration for the U^{2+} ion in $[U(Cp'')_3]^-$ ($Cp'' = C_5H_3\text{-}(SiMe_3)_2$) complex.[17] In both of these cases, the ligand field is strong enough and isotropic enough to destabilize the 7s orbitals well above the 6d orbitals, and the 5f orbitals are still as high in energy as 6d orbitals to be used to host the metal-based electron. A further complication in determining the electronic structures of the low-valent early actinides is expected to arise because when valence orbitals' energy levels of low-valent Np are in a narrow range and are not fully filled, there is usually obvious destruction of the Aufbau principle in any DFT method. For example, in the case of low oxidation state Np, placing the added electrons in the f_0 orbital will result in the unoccupied $f_{\pm3}$ orbital below the f_0 orbital. Contrary to expectations, if the electron is placed in the $f_{\pm3}$ orbital, the unoccupied f_0 orbital is below the $f_{\pm3}$ orbital.[18] To avoid these problems and to give a quantitative description in the 7s, 6d and 5f orbital energies, we have used the approximation of "smearing" in which the electrons that lie around the Fermi level and that are close in energy are smeared out over the orbitals, which are fractional occupations and mainly depends on the major quantum and angular momentum. The calculated energies of 5f, 6d and 7s atomic orbitals of Np(0) to Np(VII) are displayed in Scheme 1, which shows regular periodic trends in the valence orbitals of Np^{n+} as *n* proceeds from 0 to 7. In Np(0) and Np(I), in essence, the three orbitals are almost degenerate with the 6d being the highest energy level. Thus, our calculation of the s^1f^5 state for the Np(I) molecule **Np_2O** is reasonable. Starting from Np(II), the 5f level has declined below of 7s level and still degenerated to the 7s level, where the 6d orbitals retain higher energy than the 7s orbitals. Thus, Np has the electronic configuration of s^1f^4 or f^5 in **Np_2O_2**.[19] At Np(III), the 6d and 7s switched energetic levels, however, their energies are still near-degenerated, both being higher than 5f levels. Consequently, Np_2O_3 has the Np (f^4) configuration. As Np oxidation proceeds through the series, the valence orbitals drop in energy with the dropping in the range of 5f > 6d > 7s. This decreasing extent in the energy for different angular momentum enlarges the range of 7s, 6d, and 5f energy levels, and makes the

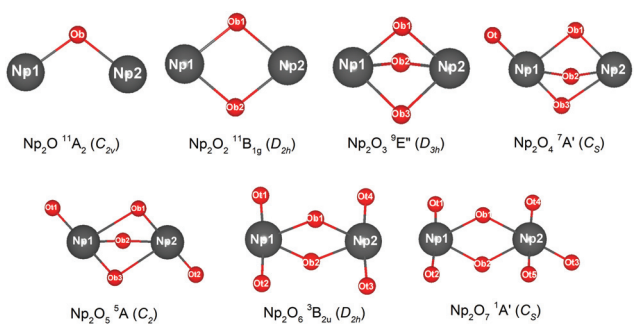

Fig. 1 The global minimum structure of Np_2O_x (x = 1 to 7).

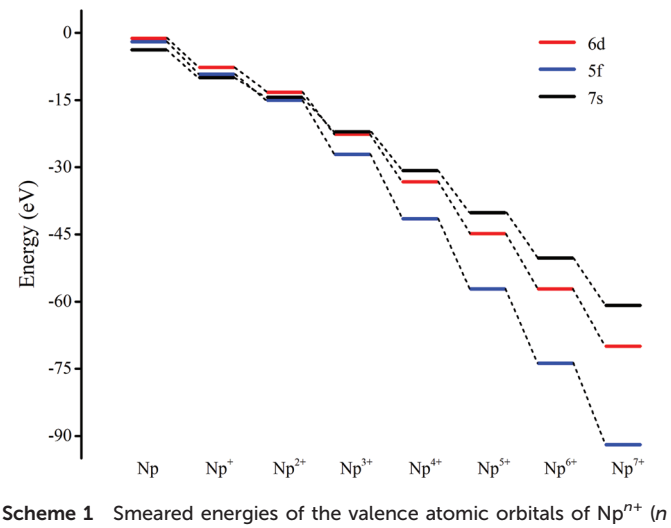

Scheme 1 Smeared energies of the valence atomic orbitals of Np^{n+} (n = 0 to 7).

5f orbitals much inert for the higher oxidation state. Thereofore, more electron-transfer from neptunium to the ligand becomes more difficult, thus making the unpaired electrons largely located on the nonbonding 5f AOs with increasing formal charge, with the number of electrons decreasing.

For instance, our calculations indicate that the ground state electronic configuration of the Np^{2+} ion in Np_2O_2 is $5f^47s^1$,[28] which differs from the Np^{2+} $5f^46d^1$ electronic configuration in the $[Np(Cp'')_3]^-$ complex,[17] in contrast to the $5f^36d^1$ configuration for the U^{2+} ion in $[U(Cp'')_3]^-$,[20] or the configuration of $5f^6$ state for Pu^{2+} in the $[Pu(Cp'')_3]^-$.[21] This is ascribed to the short Np–O bond length arouses strong interaction to destabilize the 6d orbital above the 7s orbitals. As traversing the series of oxidation states, the Np 5f orbitals gradually decrease in energy levels and become less chemically accessible, thereby the $5f^{n+1}$ configuration for trivalent Np has been presumed to have more stability. Thus, the predicted Np^{3+} ion with a $5f^4$ electron configuration in **Np_2O_3** is reasonable. Remarkably, **Np_2O_4** consists of a $5f^2$ electronic configuration of one of the neptunium centers as well as a $5f^4$ electronic configuration of the other neptunium, being capable of indicating the formation of the first mixed-valent Np^{3+}/Np^{5+} oxide compound. The reason for the formation of such an electronic structure is that Np^{5+} with double-degenerated f^2 configuration has extreme stability over that of Np^{4+} with triple-degenerate f^3 configuration, due to the lower energy levels of Np^{5+} with 5f orbitals having stronger covalence with O 2p orbitals, which is necessary for forming Np(v)═O multiple bonds. Therefore, **Np_2O_5** has a $(5f_{Np1})^2$–$(5f_{Np2})^2$ valence configuration with two pentavalent Np, which could be considered as the fifth oxygen atom consequently oxidizing the Np2(III) atom in **Np_2O_4** into Np2(v). This mechanism is evocative of the stabilization of Np(v). The ground state **Np_2O_6** is a triplet $^3B_{2u}$ state with the electronic structure of $5f^1$–$5f^1$ on Np atoms, thus each Np has a hexavalent oxidation state. For **Np_2O_7**, the lowest stable isomer is a closed-shell singlet $^1A'$ with the valence electronic structure of $5f^0$ on Np, thus a compound featuring heptavalent Np has been predicted. In addition, the series of Np_2O_x considered currently is in a neutral state and the valent state of the Np_2O_x compound indeed significantly affect the electronic structure of the Np atom, which will be discussed in our further works.

The effective charge analyses (Table S10†) show that the charge value on Np in Np_2O_x compounds increases gradually, implying that the increased oxidation state along with the increased number of oxygen atoms, agrees well with the decreasing spin population values in this series. As detailed in Table 1, the 5f population for both Np in Np_2O is $5.45|e|$, which generally decreases when x increases and becomes $5.14|e|$ in Np_2O_2 (f^5), $4.16|e|$ in Np_2O_3 (f^4), $2.53|e|$ (f^2) and $3.92|e|$ (f^4) for Np_2O_4, $2.23|e|$ for Np_2O_5 (f^2), and $1.15|e|$ for Np_2O_6 (f^1) and $0.00|e|$ in Np_2O_7 (f^0). This is a piece of evidence that the oxidation state of Np has increased from +I to +VII, as expected. Obviously, Np atoms in Np_2O_4 exhibits two oxidation states, +v in Np1 and +III in Np2, ascribed to the stable Np(v) electronic state. In addition, the trend of Bader charges on Np in Np_2O_x compounds exhibit a decreasingly enlarging trend, from $0.63|e|$ in Np_2O to $2.79|e|$ in Np_2O_7, and not linearly correlated with the oxidation state of Np, which is because a very high OS metal cation in compounds would spontaneously oxidize its ligands by self-reduction. The stabilities of the various oxidation states of Np along the series are shown in Fig. 2, where the formal oxidation states, are plotted together with the corresponding values for the HOMO–LUMO gaps.

2.2. f–f bond in Np_2O_3

Fig. 3 illustrates the linear synchronous transit (LST) potential energy surfaces of Np_2O_3 species upon converting a $^9E''$ to the $^7E''$ state as a function of the distance (R_n) from two Np centers

Table 1 Optimized structures (bond length in Å and bond angle in °), the oxidation state of Np (OS), Mayer bond order (BO) for Np1–Np2, Bader charges (Q_{Np}) as well as Mulliken spin (S_{Np}) on Np atoms of the global minimum isomer for Np_2O_x (x = 1 to 7)

Species	$^{2S+1}\Lambda$ (symm.)	Elec. conf.	OS	Geometry	BO	Q_{Np}	S_{Np}
Np_2O	$^{11}A_2(C_{2v})$	f^5s^1–f^5s^1	I–I	Np–O = 2.063 Np1–Np2 = 3.481 Np1–O–Np2 = 105.7	1.51	0.63	5.45
Np_2O_2	$^{11}B_{1g}(D_{2h})$	$f^4f^5s^1$	II–II	Np–O = 2.086 Np1–Np2 = 3.260 O1–O2 = 2.603 Np1–O–Np2 = 101.5	0.77	1.20	5.14
Np_2O_3	$^9E''(D_{3h})$	f^4–f^4	III–III	Np–O = 2.105 Np1–Np2 = 2.943 O–O = 2.603 Np1–O–Np2 = 86.6	0.55	1.75	4.16
Np_2O_4	$^7A'(C_s)$	f^2–f^4	V–III	Np1–O = 1.811, 1.972, 2.255, 2.255 Np2–O = 1.997, 2.276, 1.997 Np1–Np2 = 2.994 O_t–Np1–O_t = 179.0	0.72	2.39 1.77	2.35 3.92
Np_2O_5	$^5A(C_2)$	f^2–f^2	V–V	Np–O = 1.802, 2.103, 2.444, 1.899 Np1–Np2 = 3.105 O_t–Np–O_t = 179.0	0.31	2.42	2.23
Np_2O_6	$^3B_{2u}(D_{2h})$	f^1–f^1	VI–VI	Np–O = 2.100, 2.100, 1.792, 1.792 Np1–Np2 = 3.323 O_t–Np–O_t = 174.9	1.02	2.62	1.15
Np_2O_7	$^1A'(C_s)$	f^0–f^0	VII–VII	Np1–O = 1.787, 1.787, 2.013, 1.961 Np2–O = 1.797, 1.797, 1.846, 2.236, 2.324 Np1–Np2 = 3.493 O_t–Np1–O_t = 171.1 O_t–Np2–O_t = 166.4	0.13	2.79 2.74	0.00

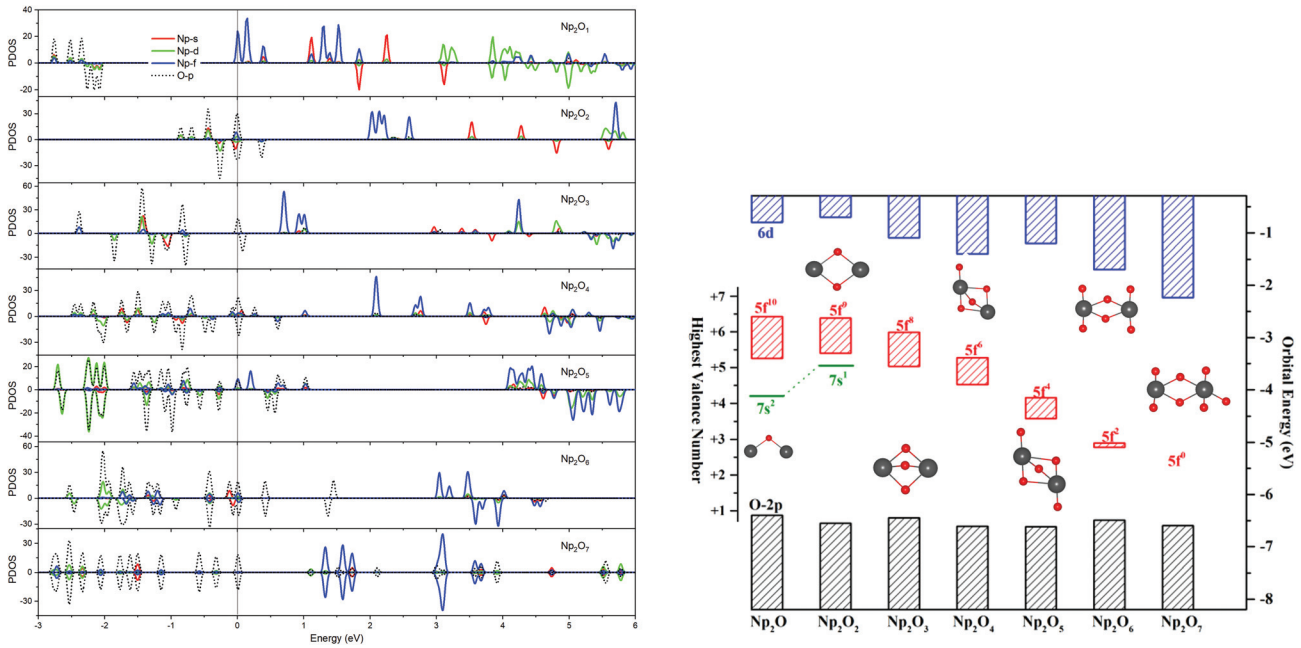

Fig. 2 The formal oxidation state of Np along with the series together with the corresponding values for the HOMO–LUMO gaps of Np_2O_x (x = 1 to 7).

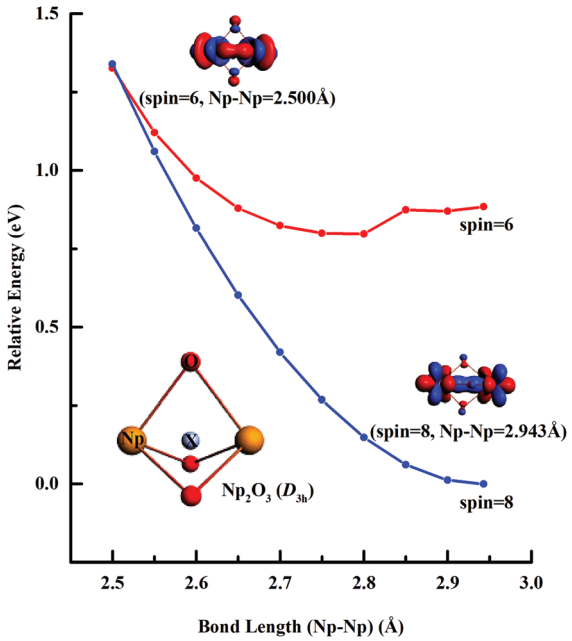

Fig. 3 Linear transit (LT) potential energy curves of Np_2O_3 calculated at the SR-DFT/PBE level.

(Np-core yellow and O-cores red) with $R_n = R_0 - 0.05n$ (n = 1–9). The starting point with R_0 = 2.943 pm corresponds to the D_{3h} structure, and the reduced ending point with R_9 = 2.500 pm, corresponds to the D_{3h} structure. Along both the potential energy surfaces, energies increase sharply before R_0 and also gradually increase after R_0, indicating that R_0 = 2.943 is the local minimum. The nonet state is generally lower in energy than the septet, while the ^{7}E″ structure with proposed f–f bonding is only slightly lower energy at R_9 = 2.500 about 0.013 eV compared to the ^{9}E″ one. Therefore, the ^{7}E″ structure is significantly less stable than the ^{9}E″ one, giving the ^{9}E″ without the f–f bond for the ground state of Np_2O_3. The intrinsic bonding mechanism in Np_2O_3 between Np and O atoms has been revealed by analyzing the Kohn–Sham molecular orbitals of Np_2O_3 and their MO energy levels with correlation to the atomic orbitals (AOs).

As illustrated in Fig. 4, the fragment molecular orbital (FMO) analysis of the Np_2O_3 (D_{3h}) ^{9}E″ ground state can be interpreted base on the orbital interactions between Np_2 and O_3 fragments. For O_3 ligands, the O 2p-based π* MOs $2b_1$, $5a_1$ and $4b_2$ play as electron acceptors when inserted into Np2, and transformed into group orbitals $7a'_1 + 6a''_2 + 1a'_2$ of the Np_2O_3. According to the frontier occupied MOs shown in Fig. 3, the splitting of Np valence orbitals upon interacting with O 2p is consistent with the conventional crystal-field theory. Without spin–orbit coupling, firstly, the 7s orbitals as doubly-occupied orbitals are σ_g in a D_{2h} field in Np_2 dimer species that is considerably further destabilized by the strong interaction with the O 2p orbitals to be unoccupied $10a'_1$ orbital. Similarly, Np 5f orbitals are split as ϕ_u (fϕ) ~ δ_u (fδ) ≪ π_u (fπ) < σ_u (fσ) in Np_2 species, where the strong destabilization of the f_σ, f_δ and f_π orbitals from the f-manifold is an indication of their strong interaction with the unfilled O 2p orbitals. Several MOs with the low orbital energies shown in the plot reflect the strong bonding interaction between the central Np 5f hybrid orbitals and O 2p orbitals; the σ_u of Np_2 overlaps with the corresponding two O $2p_z$ orbitals, forming $8a'_1$ bonding orbitals and $8a''_2$ anti-bonding orbital of Np_2O_3. The π_u group orbitals of Np_2 transform into 8e′ and 6e″ orbitals of

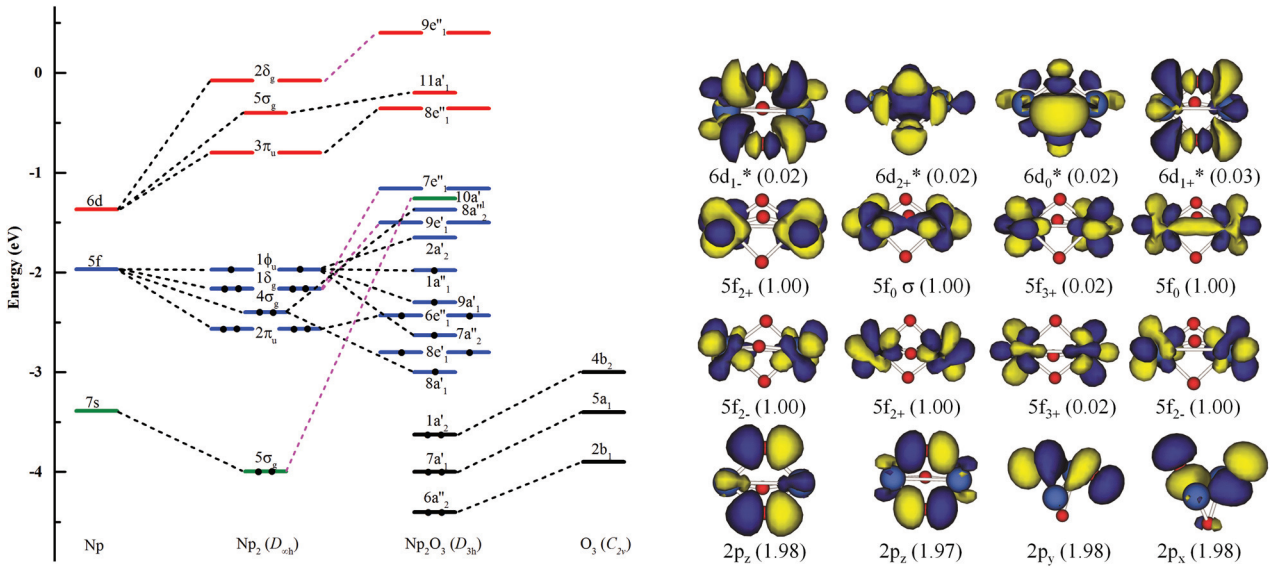

Fig. 4 Kohn–Sham MO analysis of the Np_2O_3 based on SR-ZORA PBE/TZ2P calculations. The left side is the frontier energy levels, including 6s and 5d bands; the inset on the right side is the O_3 π* levels. Np_2O_3 orbitals predicted by CASSCF (16, 16) for the nonet state along with the occupation number of orbitals.

Np_2O_3. The δ_u group orbitals of Np_2 were destabilized by the corresponding 2p orbitals of O3 π*, forming 9e′ and $7e''_1$ antibonding orbitals. The ϕ_u group orbitals of Np_2 possess as nonbonding orbitals ($7a''_2$, $9a'_1$, $1a''_1$ and $2a'_2$) of Np_2O_3. Consequently, the strong f_δ/d_δ–π* orbital interactions play a key role in stabilizing the complex. In addition, we chose the localized equivalent molecular orbital picture of Np_2O_3 (Fig. 4) based on CASSCF calculations to sketch the correlated and spin–orbit coupled valence electronic structure of ligated Np–O3–Np. Inspection of the CASSCF wave function shows that Np_2O_3 is mainly single-configurational, with a 96% dominant configurational ($(O_{2p})^8(Np_{5f})^8$) weight and 1% weight for the configuration-($(O_{2p})^8(Np_{5f})^6(Np_{6d})^2$). Since, the most stable spin state of the Np_2O_3 complex is the nonet state, among the eight unpaired electrons, which are localized on Np 5f orbitals, we observe the presence of two half-a-bond (Fig. 5) and the singly occupied σ-type orbitals containing significant contributions from both Np $5f_{z3}$ orbitals. The Np–Np interactions are characterized by a BO_{Mayer} of 0.55 from PBE calculations (comparable to 6.89 for the Np═Np double bond in Np_2), which substantiates the Np–Np single bond character. Each Np forms a strong σ-bond to the central O_3^{6-} unit through the covalent overlaps of hybridized Np (5f6d) orbitals with O(2s2p) hybrids. Each Np–O bond of dominant π-character can be described as three-center two electrons (3c–2e) bonds that possess some σ-admixture. The large electronegativity difference between Np (1.36) and O (3.44) (Pauling units) leads to bond-pair polarization toward O, especially for the π-type pairs, which are strongly localized on O and lead to its effective negative charge.

2.3. Mixed-valent in Np_2O_4

The mixed-valence has been encountered in a number of scientific areas,[22] and it has been considered relying on ligand field theory and qualitatively related to the extent of delocalization of the valence shell electrons. Especially in the transition-metal-containing compounds, the ligand field affects the local spin of metal atoms. The Np_2O_4 is a mixed-valent compound that could be ensured by structural and electronic structures that support the delocalization of 5f electrons in Np^{3+}/Np^{5+}, however, it depends less on the ligand field. Firstly, Np(v) cation Np(iii) has a quasi-tetrahedral type with the three Np–O single bonds of *ca.* 2.000 Å, while Np(v) exists in a [O═Np(v)═O]$^+$ fragment, where Np(v) presents an octahedral coordination type, *e.g.* O═Np bond lengths of 1.811 Å and 1.972 Å, and the bond angle O_t1–Np1–O_b3 of 178.3 deg. as well as the bond angle O_t1–Np1–O_b1/O_b2 of 105.4 deg., known as an Np(v) structural feature. In addition, Np–O_b distances are shorter at the Np(v) site than at the Np(iii). Thus, this mixed-valent cluster could be classified into a class II system,[22a] which has three bridging O_b between two Np ions of differing valences. In this bonding feature, two Np atoms are at a very close distance of 2.994 Å, which is of unprecedented structure and the oxidation state of Np. This structure identifies the stable geometry of anion compounds $Hf_2O_4^-$ and $Zr_2O_4^-$,[23] where the C_{3v} isomer has typical M–O and M═O stretching modes in IR spectra. Secondly, the atomic free valence and spin and orbital populations (Table 1) indicate two unpaired 5f-electrons on Np (v) atom and four unpaired 5f-electrons on Np(iii). We also chose the localized singly occupied molecular orbital (SOMO, Fig. 5) pictures to sketch the correlated oxidation states in Np_2O_4. That the lowest two SOMOs are from Np(v) atom and the rest four are from Np(iii), reflects that the higher oxidation state of Np has lower valence orbitals, due to the enlarging difference of spin-polarization of Np(v) and Np(iii). Thirdly, with the formation of Np(v), the bond angle transfers from bent to linear, which is largely ascribed to the 5f-participant in

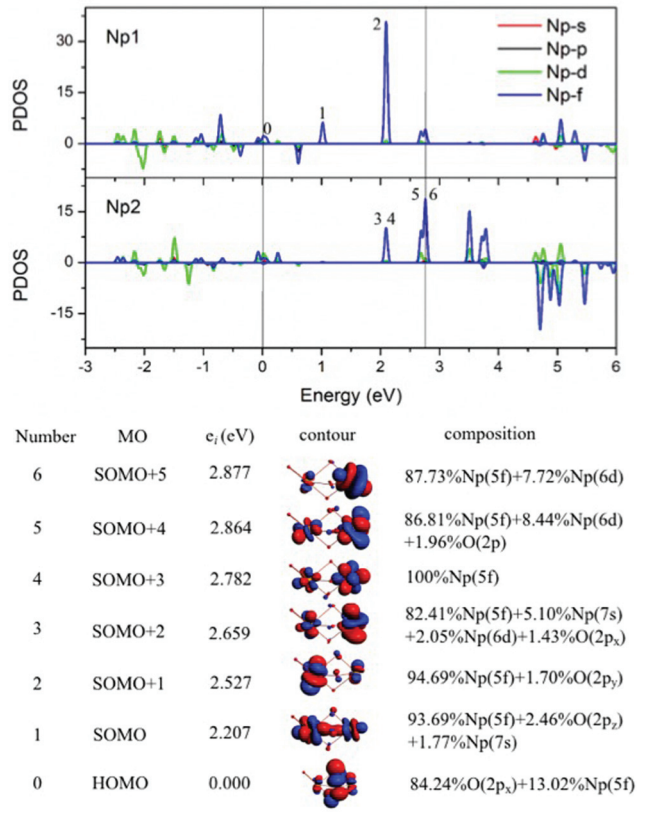

Fig. 5 Upper occupied canonical Kohn–Sham valence MO envelopes of the septet Np_2O_4 molecule. SOMO and SOMO+1 orbitals are distributed more on the Np1 atom while SOMO+2 to SOMO+5 orbitals are distributed more on the Np2 atom. The value of the contour envelopes is 0.02 a.u.

the chemical bonding of Np–O.[24] Such as one of the Np=O bonding MO in **4A** was composed of 24.85% of Np1 5f orbitals into the bonding, 6.05% larger in contribution compared to 18.80% of Np1 5f orbitals in the counterpart MO in **4C**. This phenomenon has been found as the unique feature for f-orbitals that the participation of f orbitals in chemical bonding could direct the structure of a compound.[24b] As is known, the most stable oxidation state is Np(v) and several neptunium oxidation states could exist simultaneously in the solution, thus we could provide evidence for the co-existence of two different cations (Np^{3+}, Np^{5+}) in Np_2O_4 compounds.

2.4. Heptavalent Np in Np_2O_7

In the ground $^1A'$ state for **Np_2O_7**, Np1 is bounded by three-terminal oxygen atoms with the Np1–O_{yl} bond length of 1.787 Å, by one actinyl oxygen with the Np1–O_t bond length of 1.961 Å and by one bridging oxygen with the Np1–O_b bond length of 2.013 Å, while the Np2 is bounded by three-terminal oxygen atoms with the Np2–O_t bond length of 1.797, 1.797, 1.846 Å and by one bridging oxygen with the Np2–O_b bond length of 2.236 Å. Different from the structure of U_2O_7,[25] each Np has four effectively coordinated oxygen atoms, consisting of two Np–O_b single bonds and three Np=O double bonds, which is ascribed to hexavalent U in U_2O_7 and heptavalent Np in Np_2O_7. As the investigation on the electronic structure of NpO_3 and the NpO_3^+ cation,[11c] we have known that Np is hexavalent in NpO_3 and heptavalent in NpO_3^+ cation. Thus, this Np_2O_7 structure could be understood as two quasi-planar NpO_3^+ cations connected by an O^{2-} anion, that is oxygen further oxides two Np(VI)O_3 into Np(VII) with the formation of Np_2O_7. As noted in Fig. 6, the MO diagram for Np_2O_7 in correlated to the MOs of one Np1 based NpO_3 fragment and one O fragment shows that the upper paired electrons reside in the O 2p-based MOs. For example, the O 2p-based 1a″ and 2a′ MOs are completely filled and these two MOs represent strong bonding interactions between Np 5f AOs and O 2p AOs, resulting in Np1 5f- and 6d-based antibonding orbitals (4a″ and 7a″), destabilized into a virtual band. Meanwhile, the occupied MOs are bonding orbitals with adiabatic polarization of O 2p orbitals toward the Np 5f shell, as shown from the electronic structure of MO 1a″ of Np_2O_7 in Fig. 6. In addition, the bonding between Np and the oxide within the NpO_3 fragment has significant 5f orbitals mixed into the bonding, suggesting that 5f orbitals participate in chemical bonding in the high Np compounds. Taking the Np1–O bonding orbital HOMO 3a′ as an example, that is mainly composed of 24.4% of the 5f orbitals and 76.7% of the 2p orbitals into the bonding. For Np_2O_7, the lowest 14 unoccupied MOs are mainly Np 5f character, where seven of them localized on Np1 5f orbitals are shown in Fig. 6. These wavefunction analyses clearly indicate that the Np center has an ($s^0f^0d^0$) configuration. Thus, Np has been determined as possessing an oxidation state of +VII, and the Np_2O_7 can be therefore classified as an Np(VII) species, expanding the database for heptavalent Np compounds from a monomer molecular Np(VII) complex, *e.g.* $NpO_3(NO_3)_2^-$ or

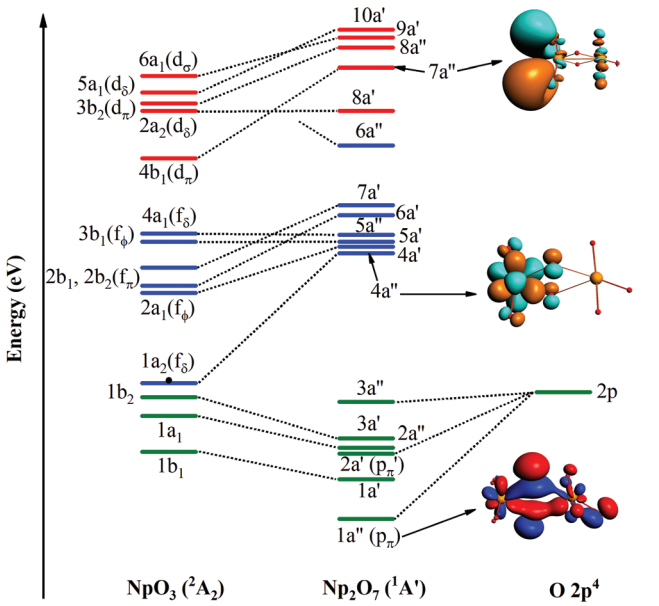

Fig. 6 Frontier canonical Kohn–Sham valence MO envelopes of Np_2O_7 with dominant AO contributions. The value of contour envelopes is 0.05 a.u.

NpO_4^-,[11a,26] to a dimer molecule, which could be considered as an example for the existence of heptavalent Np in nano-particles between the molecule and solid-state Np(VII) compounds, *e.g.* $[Co(NH_3)_6]NpO_5$ and Na_5NpO_6.[27]

3. Conclusion

We have investigated the geometry and electronic structures of the Np_2O_x (x = 1–7) species to explore how the Np oxidation state, as well as chemical bonding between Np^{n+} and O, directs the structural stability in this series. This work is intended to give several contributions in charting future directions in the neptunium chemistry with the formation of a specific oxidation state. In general, Np_2O_x provides an approach that the chemistry of radioactive Np complexes could be successfully studied *via* the combination of global-minimum search technology and relativistic quantum chemistry methods. The Np oxidation state traversing from +I to +VII shows the increased 5f-contribution to the Np–O bonding. The significant difference of Np(V) from lower oxidation states Np implies that the formation of Np(V) is extremely stable arising from the participation of 5f orbitals in chemical bonding and the ONpO linearity. Thus, the fact that mixed-valent $Np_2(III/V)O_4$ occurs between $Np(III)_2O_3$ and $Np(V)_2O_5$ is not surprising. The presently proposed $Np_2(VII)O_7$ complex with the previously reported Np(VII) compounds demonstrates that Np(VII) oxidation state is plausible in both oxides, whose stability comes from the significant interactions between O 2p orbitals and both, the Np 6d and 5f atomic orbitals. Although without spectroscopic studies on these systems, this complete computational study in both aspects of structural conformation and electronic structure corroboration, is able to provide theoretically fundamental understanding in neptunium even to the extent of early actinide elements and provide some guidance for actinide chemistry.

Conflicts of interest

There are no conflicts to declare.

Acknowledgements

This work is supported by grants from the National Natural Science Foundation of China (No. 21976014 and U1930402) and the Science Challenge Project of China (No. TZ2018004). We are very grateful to the Tianhe2-JK for generous grants of computer time.

References

1 (*a*) J. Ibers, *Nat. Chem.*, 2010, **2**, 996–996; (*b*) Z. Zheng and P. C. Burns, *Recent development in clusters of rare earths and actinides: chemistry and materials*, Springer, 2017; (*c*) P. L. Arnold, M. S. Dutkiewicz and O. Walter, *Chem. Rev.*, 2017, **117**, 11460–11475.
2 G. Tian, J. Xu and L. Rao, *Angew. Chem.*, 2005, **117**, 6356–6359.
3 (*a*) S. E. Gilson, P. Li, J. E. Szymanowski, J. White, D. Ray, L. Gagliardi, O. K. Farha and P. C. Burns, *J. Am. Chem. Soc.*, 2019, **141**, 11842–11846; (*b*) K. E. Roberts, T. J. Wolery, C. E. Atkins-Duffin, T. G. Prussin, P. G. Allen, J. J. Bucher, D. K. Shuh, R. J. Finch and S. G. Prussin, *Radiochim. Acta*, 2003, **91**, 87–92.
4 R. Husar, R. Hübner, C. Hennig, P. M. Martin, M. Chollet, S. Weiss, T. Stumpf, H. Zänker and A. Ikeda-Ohno, *Chem. Commun.*, 2015, **51**, 1301–1304.
5 (*a*) P. J. Hay and R. L. Martin, *Los Alamos Sci.*, 2000, **26**, 382–391; (*b*) J. Autschbach, N. Govind, R. Atta-Fynn, E. J. Bylaska, J. W. Weare and W. A. de Jong, *Computational methods in lanthanide and actinide chemistry*, 2015, pp. 299–342; (*c*) T. Saue and L. Visscher, *Computational methods in lanthanide and actinide chemistry*, 2015, pp. 55–87.
6 L. Zhang, E. A. Dzik, G. E. Sigmon, J. E. S. Szymanowski, A. Navrotsky and P. C. Burns, *J. Nucl. Mater.*, 2018, **501**, 398–403.
7 (*a*) R. Copping, V. Mougel, C. Den Auwer, C. Berthon, P. Moisy and M. Mazzanti, *Dalton Trans.*, 2012, **41**, 10900–10902; (*b*) S. M. Cornet, L. J. L. Häller, M. J. Sarsfield, D. Collison, M. Helliwell, I. May and N. Kaltsoyannis, *Chem. Commun.*, 2009, 917–919.
8 B. W. Veal, D. J. Lam and H. Diamond, *Physica B+C*, 1977, **86–88**, 1193–1194.
9 A. Kovács and R. J. M. Konings, *J. Phys. Chem. A*, 2011, **115**, 6646–6656.
10 (*a*) Y. Yang, H. Liu and P. Zhang, *J. Chem. Phys.*, 2016, **144**, 184304; (*b*) R. G. Denning, *J. Phys. Chem. A*, 2007, **111**, 4125–4143; (*c*) C. Zhang, S.-X. Hu, H.-T. Liu, Y. Yang and P. Zhang, *J. Phys. Chem. A*, 2018, **122**, 4085–4091.
11 (*a*) J. K. Gibson, W. A. de Jong, P. D. Dau and Y. Gong, *J. Phys. Chem. A*, 2017, **121**, 9156–9162; (*b*) P. D. Dau, R. Maurice, E. Renault and J. K. Gibson, *Inorg. Chem.*, 2016, **55**, 9830–9837; (*c*) A. Kovács, *Struct. Chem.*, 2020, **31**, 1247–1271.
12 Y. Wang, J. Lv, L. Zhu and Y. Ma, *Comput. Phys. Commun.*, 2012, **183**, 2063–2070.
13 (*a*) J. P. Perdew, K. Burke and M. Ernzerhof, *Phys. Rev. Lett.*, 1996, **77**, 3865; (*b*) E. Van Lenthe and E. J. Baerends, *J. Comput. Chem.*, 2003, **24**, 1142–1156; (*c*) B. Himmetoglu, A. Floris, S. de Gironcoli and M. Cococcioni, *Int. J. Quantum Chem.*, 2014, **114**, 14–49.
14 Y. Guo, C. Riplinger, D. G. Liakos, U. Becker, M. Saitow and F. Neese, *J. Chem. Phys.*, 2020, **152**, 024116.
15 L. Maria, J. Marçalo and J. K. Gibson, *Encyclopedia of Inorganic and Bioinorganic Chemistry*, 2011, pp. 1–13.
16 D. P. Halter, C. T. Palumbo, J. W. Ziller, M. Gembicky, A. L. Rheingold, W. J. Evans and K. Meyer, *J. Am. Chem. Soc.*, 2018, **140**, 2587–2594.
17 J. Su, C. J. Windorff, E. R. Batista, W. J. Evans, A. J. Gaunt, M. T. Janicke, S. A. Kozimor, B. L. Scott, D. H. Woen and P. Yang, *J. Am. Chem. Soc.*, 2018, **140**, 7425–7428.

18 C. E. Kefalidis, L. Castro, A. Yahia, L. Perrin and L. Maron, in *Computational Methods in Lanthanide and Actinide Chemistry*, John Wiley & Sons Ltd Chichester, UK, 2015, pp. 343–373.
19 X. Cao and M. Dolg, *Mol. Phys.*, 2003, **101**, 961–969.
20 F. S. Guo, N. Tsoureas, G. Z. Huang, M. L. Tong, A. Mansikkamäki and R. A. Layfield, *Angew. Chem., Int. Ed.*, 2020, **59**, 2299–2303.
21 C. J. Windorff, G. P. Chen, J. N. Cross, W. J. Evans, F. Furche, A. J. Gaunt, M. T. Janicke, S. A. Kozimor and B. L. Scott, *J. Am. Chem. Soc.*, 2017, **139**, 3970–3973.
22 (*a*) M. B. Robin and P. Day, in *Advances in inorganic chemistry and radiochemistry*, Elsevier, 1968, vol. 10, pp. 247–422; (*b*) S. K. Cary, S. S. Galley, M. L. Marsh, D. L. Hobart, R. E. Baumbach, J. N. Cross, J. T. Stritzinger, M. J. Polinski, L. Maron and T. E. Albrecht-Schmitt, *Nat. Chem.*, 2017, **9**, 856–861; (*c*) L. Chen, T. Zheng, S. Bao, L. Zhang, H. K. Liu, L. Zheng, J. Wang, Y. Wang, J. Diwu and Z. Chai, *Chem. – Eur. J.*, 2016, **22**, 11954–11957; (*d*) V. Dugaev, *Inorg. Mater.*, 2000, **36**, 524–526; (*e*) E. Epifano, M. Naji, D. Manara, A. Scheinost, C. Hennig, J. Lechelle, R. Konings, C. Guéneau, D. Prieur and T. Vitova, *Commun. Chem.*, 2019, **2**, 1–11; (*f*) P. Riseborough and J. M. Lawrence, *Rep. Prog. Phys.*, 2016, **79**, 084501; (*g*) D. Schweinfurth, Y. Rechkemmer, S. Hohloch, N. Deibel, I. Peremykin, J. Fiedler, R. Marx, P. Neugebauer, J. van Slageren and B. Sarkar, *Chem. – Eur. J.*, 2014, **20**, 3475–3486.
23 S. Li and D. A. Dixon, *J. Phys. Chem. A*, 2010, **114**, 2665–2683.
24 (*a*) E. Lu, S. Sajjad, V. E. Berryman, A. J. Wooles, N. Kaltsoyannis and S. T. Liddle, *Nat. Commun.*, 2019, **10**, 1–10; (*b*) S.-X. Hu, P. Zhang, E. Lu and P. Zhang, *Inorg. Chem.*, 2020, **59**, 18068–18077.
25 S. O. Odoh, J. Shamblin, C. A. Colla, S. Hickam, H. L. Lobeck, R. A. K. Lopez, T. Olds, J. E. S. Szymanowski, G. E. Sigmon, J. Neuefeind, W. H. Casey, M. Lang, L. Gagliardi and P. C. Burns, *Inorg. Chem.*, 2016, **55**, 3541–3546.
26 P. D. Dau, R. Maurice, E. Renault and J. K. Gibson, *Inorg. Chem.*, 2016, **55**, 9830–9837.
27 (*a*) V. Spitsyn, A. Gelman, N. Krot, M. Mefodiyeva, F. Zakharova, Y. A. Komkov, V. Shilov and I. Smirnova, *J. Inorg. Nucl. Chem.*, 1969, **31**, 2733–2745; (*b*) A. L. Smith, A. Hen, P. E. Raison, E. Colineau, J.-C. Griveau, N. Magnani, J.-P. Sanchez, R. J. Konings, R. Caciuffo and A. K. Cheetham, *Inorg. Chem.*, 2015, **54**, 4556–4564.
28 P. Zhang, W.-L. Zou, P. Zhang and S.-X. Hu, *Eur. J. Inorg. Chem.*, 2021, DOI: 10.1002/ejic.202100444.